VARIABILITY OF SPECTRAL SOLAR IRRADIANCE FROM VIRGO/SPM OBSERVATIONS

C. Fröhlich and C. Wehrli

Physikalisch-Meteorologisches Observatorium Davos, World Radiation Center, CH 7260 Davos Dorf, Switzerland

ABSTRACT

The VIRGO SPM on SOHO monitor spectral irradiance at 402, 500 and 862 nm with a 5 nm bandwidth. The long-term behaviour of the operational channels is dominated by instrumental degradation masking the solar variability signature. However, comparisons with the back-up channels allows to take off some of the instrumental long-term variation, and the resulting time series can now provide reliable information about variability with periods up to about a year. Time series with the long-term variation removed and the corresponding periodogram show many similarities between the three channels and total solar irradiance. Details about the spectral redistribution during changes of TSI are investigated by multivariate spectral analysis.

Key words: Spectral Solar Irradiance; Solar Variability.

1. INTRODUCTION

Spectral solar irradiance in the near UV, visible and near IR range were observed with sunphotometers (SPM) by several stratospheric balloon experiments between 1980 and 1998 and during the following space experiments: IPHIR on the Russian Mission PHOBOS, SOVA on the EURECA platform and VIRGO on the ESA/NASA mission SOHO (e.g. Brusa et al. 1983; Toutain & Fröhlich 1992; Romero et al. 1994; Fröhlich et al. 1997). These data were mainly used for helioseismic studies and the study of irradiance variability was not really possible because of the lack of long-term stability of the sensors on the missions before SOHO. The SPM data from VIRGO/SOHO have been used to determine variations on rotational time scales by Pap et al. (1999) and Pap et al. (2002). Here we report on an analysis of the instrumental long-term changes which allow to asses solar variability in the three channels for periods shorter than about a year.

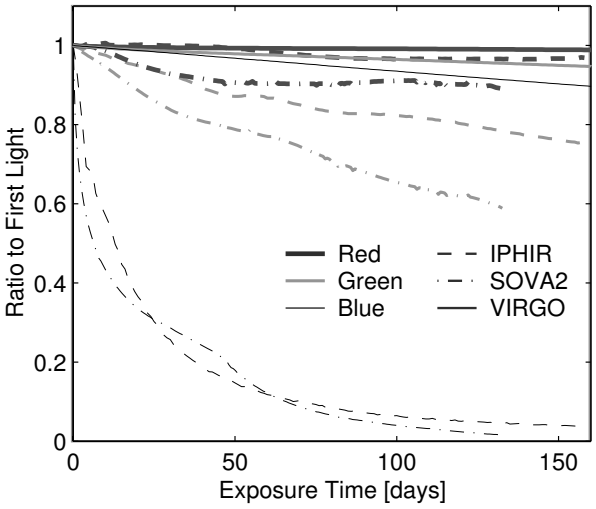

Figure 1. Degradation of SPM instruments in 3 different space experiments. IPHIR and SOVA2 had the same type of detectors and show a rapid deterioration of the UV channel. Degradation of the visible channels differs, probably due to different cleanliness of the spacecraft and their environment. Clearly, the new filters in VIRGO and strict cleanliness control of SOHO resulted in much better stability. It should also be noted that on SOHO the sensitivity of the blue channel is still at more than 30% of its initial value after nearly 6 years in space.

2. INSTRUMENTATION

The VIRGO sunphotometers (SPM) are filterradiometers with three channels of 5 nm bandwidth centered at 402, 500 and 862 nm using interference filters and silicon detectors. Two apertures of 3.0 and 6.9 mm diameter on each channel define the radiometric area and the view geometry (4° full and 1° slope angle). The filters and detectors are heated to a few degrees above ambient temperature to reduce condensation of gaseous contaminants on the optical surfaces. An additional radiation-hard glass window protects the filters from UV radiation below 380 nm. The optical compartment, sealed by O-rings and an airtight cover, was permanently flushed with pure nitrogen until just before launch. Moreover, all parts were vacuum baked before assembling in order to clean them to the highest possible degree. Figure 1 illustrates the

differences in degradation achieved with differently stringent methods to maintain or not the necessary measures to keep the instrument clean during all phases of manufacturing, integration, launch and operation in space.

Both instruments in VIRGO were activated with covers still closed on 6 December 1995 for an out-gassing period until on 17 January 1996 when the cover of SPM-A was opened. Primarily a helioseismological instrument, it is operated continuously with a one-minute sampling cadence since then. SPM-B is the radiometric instrument, intended to monitor the solar spectral flux and the degradation of SPM-A. Besides, it may substitute the primary instrument in case of a failure. It was exposed briefly every 60 days until end of 1998, since February 1999 the SPM backup rate is once every 30 days. SPM measurements are corrected for temperature variations and normalized to solar irradiance at a distance of 1AU using constant radiometric calibration factors throughout the mission. Hourly and daily means for SPM-A are derived from the high cadence readings. In the present analysis we use hourly values.

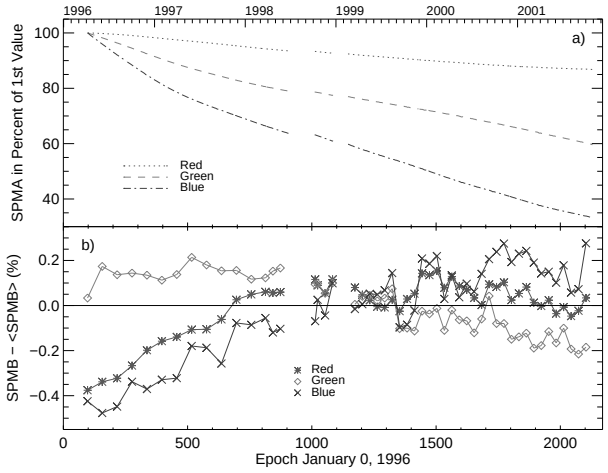

Figure 2. The upper panel shows the results from the operational SPM-A which is exposed since the beginning of the measurements in February 1996, the lower panel the results of SPM-B, the instrument which is exposed to the sun only about once a month for a few minutes.

3. DETERMINATION OF LONG-TERM CHANGES AND DETRENDING

Figure 2 shows the level1 data for the SPM-A and B on VIRGO. It is quite obvious that the results of SPM-B do not reflect solar variability, but mostly instrumental changes. The red and blue channels and to a lesser extent also the green one show a gradual increase of sensitivity during the first three years which seem to flatten out a few month before the interruption during the SOHO vacation. Then the green starts to decrease, the red stays about constant and blue is still, but less than before, increasing. Some of the early increase can also be seen in SPM-A, which is, however, mostly hidden in the general decrease. In order to correct the data we first fit to the

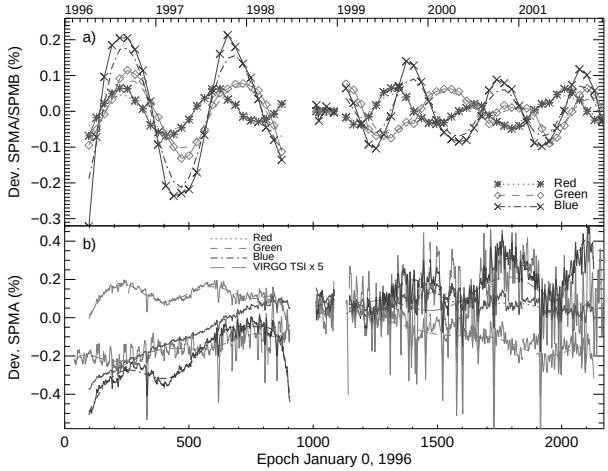

Figure 3. (a) shows the deviation from the fit to SPM-B. Note the pronounced annual oscillation the mechanism of which is not understood. (b) shows the deviation after applying the correction determined from ratioing with SPM-B. Note that the scale for the TSI is 5 times larger than the one for the SPM. So the corrections for the latter are more than 5 times larger than for TSI.

ratio of SPM-A/B a 3rd degree polynomial. The residuals from these fits (upper panel of Fig. 3) are distinct oscillations with a period close to one year. A correlation with the instrument's temperature, which has also a basic period of one year, was inconclusive. Nevertheless we apply this correction to the data and obtain flattened time series of SPM-A that follow closely the general behaviour of SPM-B as intended (see lower panel of Fig. 3). In order to detrend these 'normalized SPM-A data', we fitted them with polynomials of degree 8 as shown in Fig. 3b.

In order to assess the influence of these corrections the power spectrum is calculated and for the TSI the frequencies where the spectrum crosses the 3db line determined (Fig. 4). In the low frequency part there are three places identified at periods of 320, 175 and 122 days, respectively. As will be shown below, the lowest period is relevant for the power spectral analysis and thus is limited to periods shorter than about 4 to 5 solar rotations.

The time series of the detrended SPM-A channels are plotted together with the detrended TSI in Fig. 5. The resemblance of the four time series is remarkable. The ratios of the variance of the red, green and blue channels to TSI amount to 0.82, 1.48, and 1.93. But there are also some differences which are most visible in the time series during solar minimum, mainly because of lower solar variability. It is not yet clear whether these differences, e.g. the oscillations in the blue and green channel, are still remnants of instrumental effects or of solar origin.

4. SPECTRAL REDISTRIBUTION OF THE VARIANCE

The spectral redistribution can be determined by performing a multi-variate frequency analysis which accounts

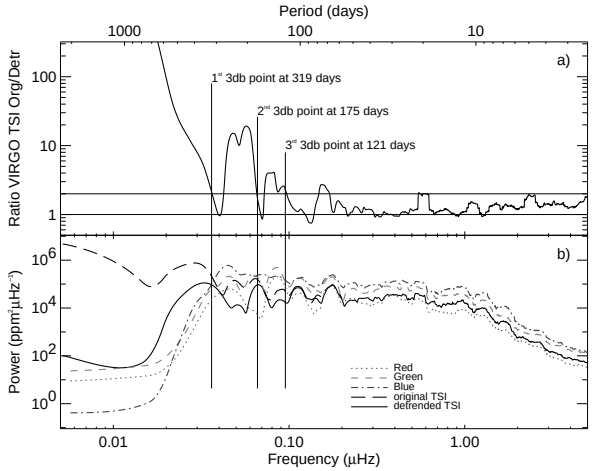

Figure 4. Power spectra of TSI and SPM: the upper panel shows the ratio of the power spectra of original and detrended TSI. The lower panel those for the three SPM channels and TSI. It is obvious that variability with periods less than an year are reliable.

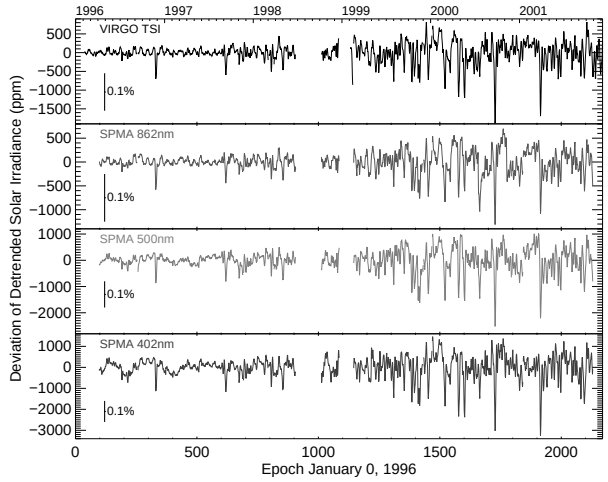

Figure 5. Time series of detrended TSI and the three channels of SPM-A.

for the influence of the time-series $X_1(t)\ldots,\ X_j(t)\ldots,\ X_m(t)$ on $Y(t)$ by constructing the linear transformation $\mathbf{L}(X_1(t)\ldots,\ X_j(t)\ldots,\ X_m(t))$ of these time series which best approximates $Y(t)$. This can be analyzed in the frequency domain of and the linear transformations become m linear spectral filters $B_j(\nu)$, determined by comparison of the spectra f_{Xj} with f_Y made frequency by frequency. The multiple coherence $\rho_j(\nu)$ is then a measure of the association between the series and $100 \times \rho_j(\nu)^2$ gives the amount in percent of the part in $Y(t)$ explained by the transformed $X_j(t)$. The total coherence $\rho(\nu)^2 = \sum \rho_j(\nu)^2$ corresponds to the total amount explained by the variance in the combination of all $X_j(t)$. The basic theory can be found in e.g. Koopmans (1974, Chapters 5.6f, 8.4f). This analysis is applied to the three SPM time series as $X_{\rm R}$, $X_{\rm G}$ and $X_{\rm B}$ and the TSI time series as Y . The results for of the coherence, gain and phase are shown in Fig. 6 and in Table 1.

The low frequency part of the cross correlations are influenced by the way the detrending is performed. Polynomial fits do not only influence the amplitude, but also the phase. From the plots of the coherence we conclude that the information below about 0.09 μHz (period of $\approx$130 days) is more and more contaminated by the detrending. This is at about a 3 times higher frequency than concluded from Fig 4 which was based on a simple 3db amplitude argument. At low frequencies the blue and red are contributing lesser to the variance of TSI than the green channel. It is generally accepted that the slow variations of TSI are mainly due to changes in the UV (up to 30% of the variance) and the observed decrease is somewhat puzzling and may still be due to the data treatment. At periods below about 70 days there are interesting features as the one at the 27-day solar rotation where a wide peak in the red fills in the dip in the blue. Another, even more pronounced sequence is at periods around 20 and 10 days where the green takes over from the blue. Or, the one at 13 days where, as for the 27-day period, the red compensates for the loss in the blue. This is indeed astounding as the UV irradiance has a strong 27-day modulation, which may, however, be mainly due to the strong lines whereas the blue channel at 402 nm is more representative for the continuum. Variations in three channels explain 97% of the variance of total solar irradiance, with contributions of 13% from the red , 26% from the green and 58% from the blue, respectively. The spectral redistribution is shared by the red, green and blue as 1.0 : 2.2 : 4.8. The gain - the factor by which the

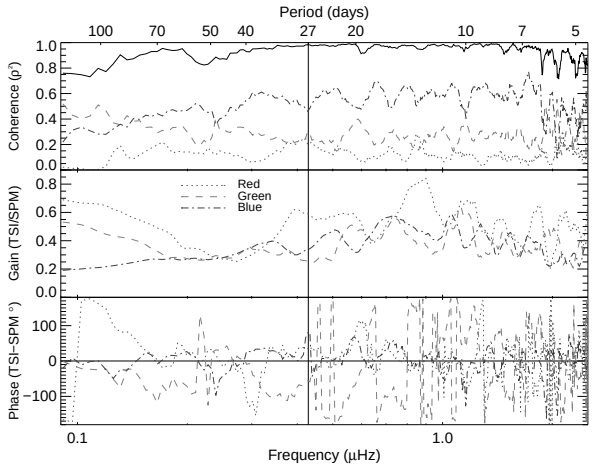

Figure 6. Results of the multivariate spectral analysis for the three SPM times series against the TSI time series. The top panel shows the coherence ρ_j^2, the middle the gain and the bottom one the phase of the linear filter.

Table 1. Summary of the coherence, gain and phase as average over the spectral range $0.289\ldots1.653\mu$*Hz (periods* $7\ldots40$ *days).*

channel	ρ^2	gain	phase (deg)
red	12.2 %	0.57	4.7
green	26.4 %	0.41	-14.1
blue	58.3 %	0.42	2.3

SPM reading has to be multiplied to get the TSI signal - is in general higher for the red, the green and blue on the other hand are about the same as listed in Table 1. The phase – the least reliable part of the linear filter because of its ambiguity of $\pm\pi$ – indicates with a positive sign a phase lead of the SPM relative to TSI. Up to frequencies of about 0.2 μHz (period of $\approx$60 days) the green and blue channels are more or less constant whereas the red seems to turn around; at higher frequencies the green changes more than the blue and red. The rather small average values as listed in Table 1 are probably not significantly different from zero. Finally, Fig. 7 shows the share of the power of TSI explained by the three channels.

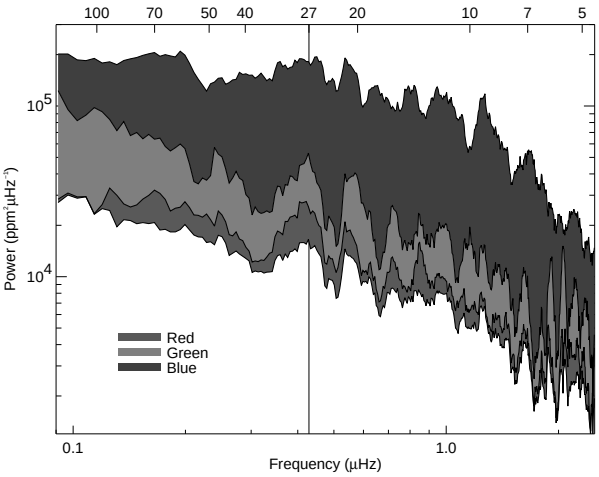

Figure 7. Results of the multivariate spectral analysis for the three SPM times series against the TSI time series displayed as shares of the TSI power spectrum. The explained part covers about one order of magnitude which corresponds to the 97% in the range $0.289 \ldots 1.653 \mu Hz$ *(periods* $7 \ldots 40$ *days).*

5. CONCLUSIONS

The long-term trends of the SPM are not understood well enough to assess the solar cycle variability of the spectral channels. From the spectral analysis of the detrended time series the 3 db points of the high-pass filter are at periods of 320, 175 and 122 days, respectively. A closer look at the coherence determined from a multivariate frequency analysis, however, suggests that the spectra are reliable only for periods less than about 130 days. This allows to assess details of the variability in the range of up to 5 solar rotation periods. In this range 97% of the variance of TSI can be explained by the combination of the red, green and blue channel with a spectral redistribution ratio of 1.0 : 2.2 : 4.8. Interesting information is gathered about the change of the share at the 27-day rotational period and its first harmonic, indicating that the red part of the spectrum seems to influence this modulation more than the blue.

ACKNOWLEDGMENTS

We would like to thank the Swiss National Science Foundation for support of the VIRGO Project at PMOD/WRC. These results would not be possible without the continuous efforts of the VIRGO and SOHO teams. SOHO is a cooperative ESA/NASA mission.

REFERENCES

Brusa R.W., Fröhlich C., Wehrli C., 1983, In: Kopp E. (ed.) Sixth ESA Symposium on European rocket and balloon Programmes, 429–433, ESA SP-183, ESA Publications Division, Noordwijk, The Netherlands

Fröhlich C., Crommelynck D., Wehrli C., et al., 1997, Sol. Phys, 175, 267

Koopmans L., 1974, The Spectral Analysis of Time Series, Academic Press, Inc., London, GB

Pap J., Anklin M., Fröhlich C., et al., 1999, Adv. Space Res., 215–220

Pap J., Turmon M., Floyd L., Fröhlich C., Wehrli C., 2002, Adv Space Res., in press

Romero J., Wehrli C., Fröhlich C., 1994, Sol.Phys., 152, 23

Toutain T., Fröhlich C., 1992, Astron. Astrophys., 257, 287